Epilepsia, **48**(Suppl. 4):65–74, 2007
Blackwell Publishing, Inc.

Imaging of Intrinsic Optical Signals in Primate Cortex during Epileptiform Activity

*Michael M. Haglund and †Daryl W. Hochman

*Departments of *Surgery (Neurosurgery) and Neurobiology, and †Surgery (Experimental) and Pharmacology & Cancer Biology, Duke University Medical Center, Durham, North Carolina, U.S.A.*

Summary: Localized increases in neuronal activity are known to alter the distribution and oxygen content of blood within the surrounding brain tissue. In the neocortex, these activity-evoked hemodynamic changes are predominantly mediated through the dilation of the microscopic pial arterioles that lie on the surface of the brain, nearest to the site of activation. Since hemoglobin absorbs light throughout the visible and near-infrared spectrum, optical microscopy combined with computer imaging techniques can be used to map the patterns of hemodynamic changes associated with neuronal activity. Examples of optical imaging data are provided here to demonstrate four points. First, depending on the optical wavelength chosen for illumination of the cortex, different spatial and temporal patterns of optical changes are elicited by similar stimuli yielding distinctly different types of physiological information. Second, by selecting the appropriate wavelengths, it is possible to generate maps from optical-imaging data that represent changes predominately due to either blood volume (at 535 nm) or blood oxygenation (at 660 nm). Third, "negative" optical signals are negative only relative to a given optical wavelength, and appear to be associated with more intense types of neuronal activation. Fourth, optical imaging is a useful technique for studying neocortical seizure activity in animal models, with the caveat that species-specific differences in cortical size and vascularization patterns may be important to consider in the interpretation of optical imaging data. **Key Words:** Optical imaging—Intrinsic optical signal—Epilepsy—Neocortex—Hemodynamics.

WHAT IS INTRINSIC OPTICAL SIGNAL IMAGING?

Changes in the magnitude of neuronal activity are known to alter the light scattering and absorption properties of brain tissue. In mammalian cortex, these optical changes are generated by at least three components: (i) changes in blood volume; (ii) changes in blood oxygenation; and (iii) ion-fluxes between neurons and glia and the resultant cell volume changes (Grinvald et al., 1988; Holthoff and Witte, 1996; MacVicar and Hochman, 1991). Optical changes in vivo are thought to be dominated by the first two blood-dependent components (Malonek and Grinvald, 1997; Haglund and Hochman, 2004). Since these optical changes can be measured without the use of dyes or contrast-enhancing agents, they are often referred to as "intrinsic optical signals" (IOS). IOS imaging involves the illumination of neuronal tissue with visible or near-infrared light and acquiring images with a digital video camera. Since high-resolution IOS images can only be acquired from the exposed surfaces of tissue, in vivo applications are usually restricted to mapping changes on the neocortical surface. Even given this limitation to mapping tissue surfaces, IOS imaging has been found to be useful for studying the functional organization of visual cortex (Grinvald, 1992; Martin, 2002; Schummers et al., 2004; Tanaka, 2000), and has been applied, though less frequently, to intraoperative mapping of functional and epileptiform activity in human subjects (Haglund et al., 1992; Cannestra et al., 2001; Haglund and Hochman, 2004, 2005; Sato et al., 2005 Schwartz et al., 2004). The usefulness of IOS imaging for studying cortical activity relies on the property that the IOS changes at various optical wavelengths tend to be spatially localized to where populations of neurons undergo changes in their level of activity. IOS imaging thus offers the ability to study activity-evoked changes over large areas of cortex without the need to use techniques that can potentially damage cells, such as the application of dyes which may be phototoxic, or the insertion of microelectrodes into the cortex. IOS imaging may be well suited for studying neocortical epileptiform activity in animal models, though to date relatively few studies have been published on this application (Haglund

Address correspondence and reprint requests to Daryl W. Hochman, Dept. Surgery, Box 3807, Duke University Medical, Durham, NC 27710, U.S.A. E-mail: dhochman@duke.edu
doi: 10.1111/j.1528-1167.2007.01243.x

et al., 1993; Chen et al., 2000; Schwartz and Bonhoeffer, 2001; Suh et al., 2005).

WHAT CAUSES OPTICAL CHANGES IN CORTICAL TISSUE?

An increase in neuronal activity within the neocortex is associated with a redistribution of blood volume within the vicinity of the active tissue (Mchedlishvili, 1987; Roland, 1997). These hemodynamic changes are mediated through the dilation of the pial arterioles; signaling molecules such as adenosine and nitric oxide are released by neurons as they fire action potentials and diffuse through the extracellular space, causing nearby arterioles to dilate (Ngai et al., 1988; Iadecola, 2004). Interpretation of imaging data that is derived from these activity-evoked hemodynamic changes relies on understanding how the spatial and temporal changes in the flow, volume, and oxygen-content of hemoglobin within cortical tissue vary as function of neuronal activity. Starting with the major cerebral arteries, repeated bifurcating of larger into smaller vessels that form anastomotic interconnections give rise to a complex vascular web covering the neocortical surface. It has been shown that the vessels which play the most significant role in the redistribution of hemoglobin are those segments of the smallest pial arterioles just prior to their penetration into the cortex (Mchedlishvili, 1987; Ngai et al., 1988). Pial arterioles less than 100 microns in diameter, closest to areas of increased cortical activity, have been observed to undergo significant dilation during action potential firing, with the largest dilations being associated with the smallest vessels that have resting diameters in the range of 10–30 μm. Since blood flow is approximately related to the fourth power of vessel diameter (Fung, 1997), small changes in neuronal activity are amplified into large changes in blood flow via dilation of the pial arterioles. There are two important activity-modulated hemodynamic properties that contribute to the in vivo optical signal: (i) increases in blood volume, arising from the increased diameters of the pial arterioles, and (ii) increases in blood oxygenation in the venous network, arising from the reduced transit time of hemoglobin in the cortical tissue during the dramatically increased flow velocity (Mchedlishvili, 1987; Roland, 1997).

As noted from the absorption spectra of oxy- and deoxy-hemoglobin (Fig. 1), the amount of light absorbed by blood varies as a function of the wavelength of light used for illumination. At some wavelengths, such as 525–550 nm, the light absorption properties of oxy- and deoxy-hemoglobin are nearly indistinguishable from each other (i.e., isosbestic points) and hence these wavelengths can be used to map changes in the total amount of hemoglobin that result from changes in the diameters of the microscopic pial arterioles, independent of changes in oxygen content. We therefore refer to optical changes at an isosbestic point, such as 535 nm, as a "blood volume signal." At other wavelengths, such as 660 nm, oxy- and deoxy-hemoglobin are maximally distinguishable, and hence

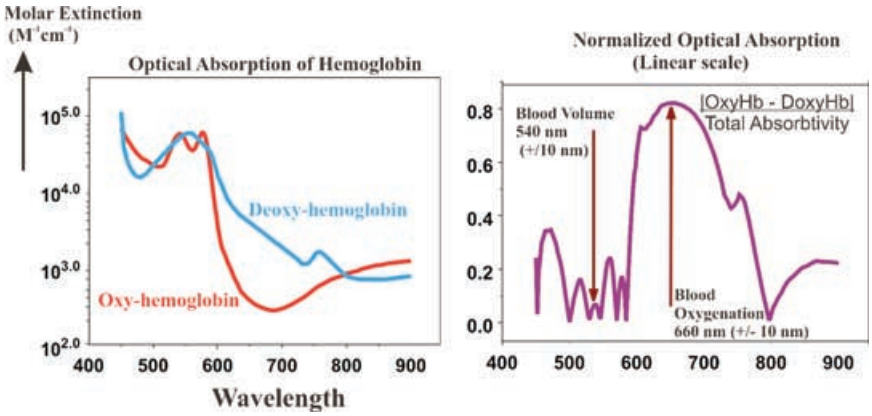

FIG. 1. Optical Absorption Properties of Hemoglobin. The left-hand plot compares the amount of light that is absorbed by oxy- and deoxy-hemglobin at wavelengths from 400 nm through 900 nm. The graphs cross at some wavelengths where oxy- and deoxy-hemoglobin absorb exactly the same amount of light, called isobestic points, and hence imaging at these wavelengths is insensitive to differences in blood oxygenation. These data are plotted against a logarithmic y-axis, making their absolute differences difficult to judge. The graph on the right is a linear plot derived from the same data. Here, the absolute difference in light absorption between oxy- and deoxy-hemoglobin (normalized by their total cumulative absorptivity) is plotted on a linear scale. Wavelengths at which oxy- and deoxy-hemoglobin are indistinguishable are those at where this difference vanishes (i.e., where the graph touches with x-axis). As can be seen in the right-hand plot, oxy- and deoxy-hemoglobin are maximally different at 660 nm, and hence this wavelength may be useful to measure changes in the oxygen content of blood. At wavelengths between 525 nm through 555 nm, oxy- and deoxy-hemoglobin are nearly indistinguishable; hence these wavelengths may be useful for measuring blood volume changes independently from blood oxygenation. These graphs were generated from publicly available data on the web compiled by Dr. Scott Prahl, Oregon Medical Laser Center at http://omlc.ogi.edu/spectra/hemoglobin/summary.html, tabulated from data by Drs. W. B. Gratzer, Med. Res. Council Labs, Holly Hill, London and N. Kollias, Wellman Laboratories, Harvard Medical School, Boston.

imaging at these wavelengths can provide a "blood oxygenation signal." An increase in neuronal activity would be expected to elicit opposite-going optical changes in the blood volume (535 nm) and blood oxygenation (660 nm) signals: (i) at 535 nm, the tissue would be predicted to become darker due to an increase in the concentration of light-absorbing hemoglobin molecules within a volume of tissue, and (ii) at 660 nm, the tissue would be predicted to become lighter, or reflect more light back to the detector, since blood oxygenation is increased in the venous network, and oxy-hemoglobin absorbs less light at this wavelength. However, this explanation is an oversimplification, since changes in the opposite directions to what was just described have been reported at these wavelengths, and their interpretation has long been debated (Malonek and Grinvald, 1996; Buxton, 2001; Lindauer et al., 2001).

METHODS FOR OPTICAL IMAGING OF PRIMATE CORTEX

The details of the treatment and preparation of primates for optical imaging studies have been previously described in detail (Haglund et al., 1993). Macaque monkeys (Macaca nemestrina) were used for all the data shown here, with their care and treatment conforming to a protocol approved by Duke's Institutional Animal Care & Use Committee. To allow for imaging and electrophysiological recordings from the neocortex, a 25 mm craniectomy over hand motor cortex is performed and a specially designed 25 mm threaded stainless steel chamber is mounted to the cranium to provide an "optical window." For electrical stimulation of the cortex, a bipolar stimulating electrode (5 mm interelectrode distance) powered by a constant-current source (Ojemann Cortical Stimulator, Integra Life-Sciences Corporation, NJ, U.S.A.) is placed on the neocortical surface.

The optical imaging equipment and data analysis methods used to generate the data presented here are identical to what has previously been described for use on human subjects (Haglund and Hochman, 2005). Briefly the cortex is illuminated with either 535 nm or 660 nm light. Images are acquired with a cooled 16-bit digital CCD camera (Roper Scientific, NJ, U.S.A.). Sequences of images are integrated over 100 ms or 200 ms intervals and stored on hard disk for offline analysis. In order to visually demonstrate the spread of stimulation-evoked optical changes over the cortex, "difference-images" are generated by subtracting a randomly chosen prestimulation image (i.e., "control-image"), acquired sometime during a 20 s interval prior to stimulation, from all of the images in its associated series. Each difference-image thus represents the absolute change in the optical signal from the chosen control image. The difference-images are then divided by the control image to provide a map of percentage change. Images are pseudo-colored to make small optical changes more apparent.

THE "AFTERDISCHARGE MODEL" OF EPILEPTIFORM ACTIVITY

Electrical stimulation of the cortex at varying currents has been used previously in human subjects to correlate optical signals to the magnitude of cortical activation (Haglund and Hochman, 2004, 2005). This technique involves stimulating the cortex with a bipolar electrode (60 Hz; 1 ms per pulse; 4 s) placed on the cortical surface (Fig. 2; bottom left grey-scale image). The stimulation-currents are initially tested at a low setting and gradually increased until a current is found that is just sufficient to consistently elicit an episode of afterdischarge (epileptiform) activity that persists after the 4 s of stimulation has ended. In this way, stimulation currents are found that allow for imaging the cortex in response to stimuli that either do, or do not, elicit epileptiform activity. For each primate cortex studied, an afterdischarge threshold was found (i.e., a minimal stimulation current that was just sufficient to elicit epileptiform activity) that reliably elicited an episode of afterdischarge activity of similar duration and intensity following each stimulation (Fig. 2, top traces); the durations and amplitudes these afterdischarge episodes have been found to remain relatively constant throughout the entire duration of each experiment for a given animal. For the studies reported here, the hand motor cortex was exposed for electrical stimulation and optical imaging. Ongoing hand-twitching movements could be clearly observed that lasted exactly as long as the electrographic afterdischarge activity. To facilitate the optical imaging studies, the recording electrodes were removed from the cortex once the afterdischarge threshold was established; thereafter, the duration of hand twitching was used as a behavioral assessment of afterdischarge activity. In the eight primates we have studied to date, afterdischarge thresholds have varied from 4 mA to 16 mA.

In what follows, we demonstrate that different patterns of optical changes occur when comparing those trials in which electrical stimulation elicits afterdischarge activity to those trials in which no epileptiform activity is elicited. One question is whether these differences are truly due to the presence of epileptiform activity, or alternatively are the consequence of the greater stimulation currents required to elicit the afterdischarge activity. We note that a small change (1 mA) in the magnitude of stimulation current determines whether or not a prolonged period (>10 s) of afterdischarge activity occurs (Fig. 2). Our experience to date is that unique optical changes occur during the presence of afterdischarge activity that are not present otherwise, even when significantly larger stimulation currents are used to study animals that have higher afterdischarge thresholds.

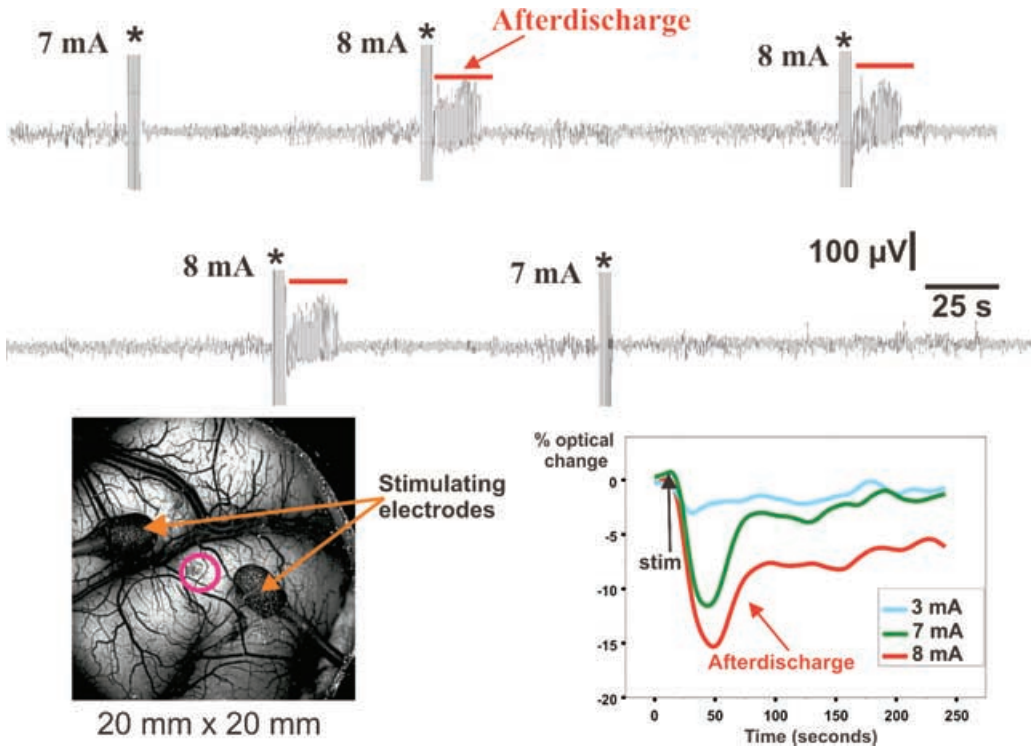

FIG. 2. The Afterdischarge Model. At the beginning of each experiment, primate hand motor cortex was stimulated with currents of increasing magnitude until a current was found that consistently elicited afterdischarge activity; this defines the afterdischarge threshold current. It is typically observed that current at 1 mA below the afterdischarge threshold fails to elicit epileptiform activity. As shown in the top continuous trace recorded from a surface electrode (not shown) placed between the two stimulating electrodes (bottom left grey-scale figure), 8 mA was just sufficient to consistently evoke afterdischarge activity in this animal. Stimulation artifacts in the top traces are marked with stars, and afterdischarge activity with orange bars. Optical changes (535 nm) of the pixel values from within the colored circle overlay in bottom left image, elicited by various stimulation currents, are shown in the bottom right graph. Note that the magnitude, the time to reach the maximum value, and the time to recover to baseline, are significantly greater for optical changes occurring during the 8 mA trial that elicited $>$ 10 seconds of afterdischarge activity as compared to the 7 mA trial in which no epileptiform activity occurred.

DISTINGUISHING CHANGES IN BLOOD OXYGENATION FROM BLOOD VOLUME WITH OPTICAL IMAGING

In the experiment shown in Fig. 3, it was found that a current of 7 mA was just below the threshold for generating epileptiform activity, and 8 mA was just above this threshold. At a sufficiently low magnification, the entire area within the recording chamber can be imaged (Fig. 3; top panel of images). Images acquired at 535 nm that immediately following the 4 s of 7 mA stimulation (Fig. 3; top left) showed the largest changes occurring within the tissue surround one of the stimulating electrodes, and no optical changes occurred within the larger blood vessels; all optical changes occurred in a negative-going direction (i.e., the tissue became darker with activation). It is typical for more current to be delivered to the tissue by just one of the two stimulating electrodes (Haglund et al., 1993), hence one of the two electrodes consistently shows a larger optical change than the other. Imaging at 660 nm showed the largest optical changes within the larger veins lying within the sulci nearby the site of electrical stimulation. At this wavelength, the optical changes at the end of the 4 s stimulation period were in a positive direction.

In order to determine the localization of the optical signal within the various microvascular compartments, imaging was performed at sufficiently high magnification to resolve the smallest pial arterioles within an area near the stimulating electrode (Fig. 3; middle panel of images). It was noted that under 535 nm light, the largest optical changes were restricted to the pial arterioles (Fig. 3, left; middle panel), and at 660 nm the largest optical changes occurred within the single venule that was within the field of view (Fig. 3, right; middle panel). The pial arteriole that showed the optical changes at 535 nm during stimulation was also observed to undergo significant vessel dilation (approximately a 35% increase from its resting diameter) that coincided with the time course of the optical changes.

In order to quantify the time course and magnitude of the optical changes at each wavelength, the percent changes of the IOS within several areas of interest were calculated and plotted as time series (Fig. 3; bottom). At 535 nm, optical changes were much larger within the tissue surrounding

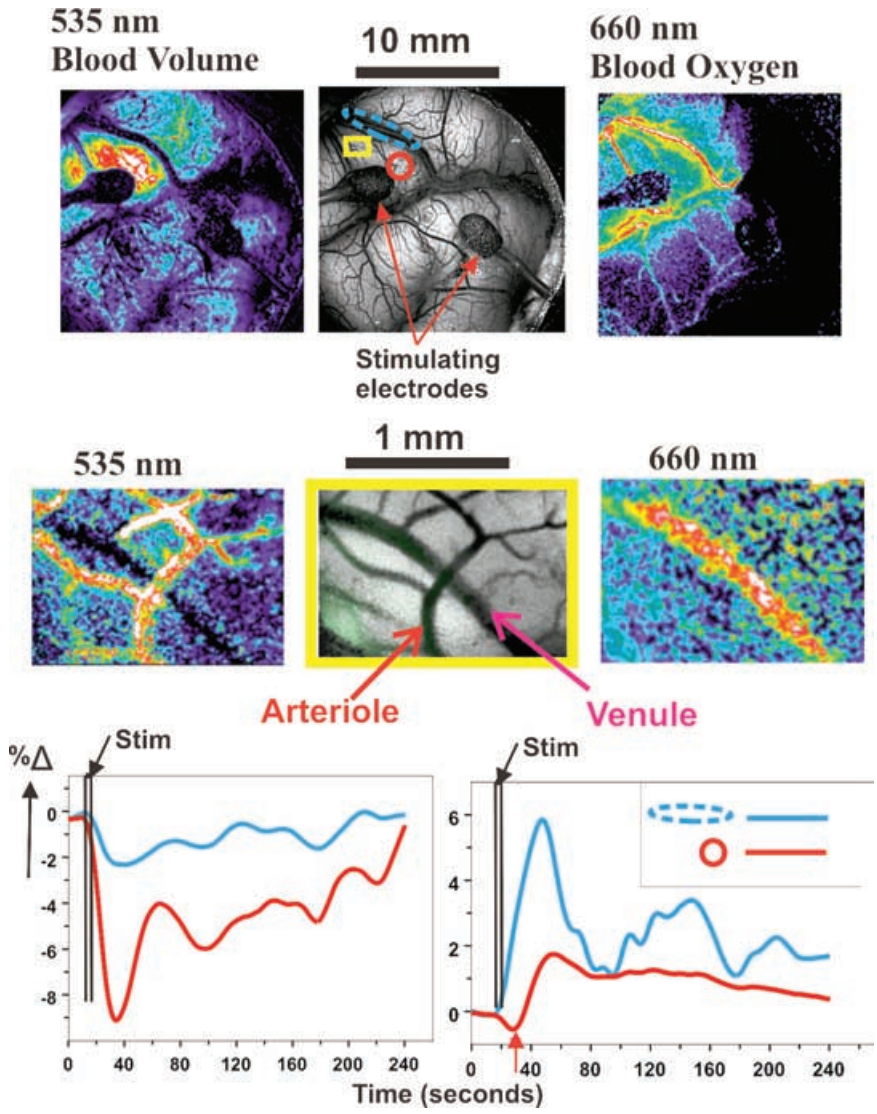

FIG. 3. Localization of Optical Changes at 535 nm and 660 nm. The top panel shows low-magnification maps of optical changes during 7 mA stimulation, where no afterdischarge activity was elicited by the stimulation. These data are from an individual animal. The middle, top grey-scale figure shows the configuration of the stimulating electrodes, and the red, yellow, and blue overlays show regions whose optical changes are plotted quantitatively in the graphs at the bottom of this figure. Images on the left and right are pseudo-colored to indicate their percent changes in the optical signal from baseline conditions. When the cortex is illuminated with 535 nm light (top, left), the largest optical changes are nearest to one of the stimulating electrodes, and distributed diffusely throughout the surrounding tissue. Under 660 nm light (top, right), the optical changes are greatest in the largest veins lying within the cortical sulci. The middle panel shows optical changes acquired at high magnification, within the area indicated by the yellow square in the top middle figure. During stimulation, the pial arteriole was observed to undergo a 35% increase in its resting diameter. 535 nm optical images (middle, left) show that optical changes are restricted to the pial arteriole, and absent from the venule. 660 nm images (middle, left) show that changes are restricted to the nondilating venule. The pial arteriole shown here is approximately 20 microns in diameter at rest, and the venule is 35 microns in diameter. Pixel values from the orange and blue overlays in the top middle figure are plotted at the bottom as a time series. At 535 nm (bottom, left), the peak changes occur approximately 15 seconds after stimulation had ceased, and were significantly larger in the tissue surround the stimulating electrode. At 660 nm (bottom, right), the changes were greatest in the venule, and their peak changes occurred approximately 25 seconds after stimulation had ceased. Note that, a slight negative dip is observed to occur in the tissue surround the electrode (indicated by the orange arrow in the bottom right graph).

the stimulating electrode (Fig. 3; bottom, left), in contrast to the signal at 660nm that showed the largest changes in a nearby large vein (Fig. 3; bottom, right). Although the signals at both wavelengths are correlated spatially to where the cortex was stimulated, and their onset times occurred simultaneously with the onset of electrical stimulation, their peak changes and durations were distinctly different. The peak of the IOS changes following stimulation at 535 nm occurred 10–15 s after the electrical stimulation had ceased, and 20–30 s after the stimulation at 660 nm. It was also noted that at both wavelengths, the stimulation-evoked optical changes took several minutes

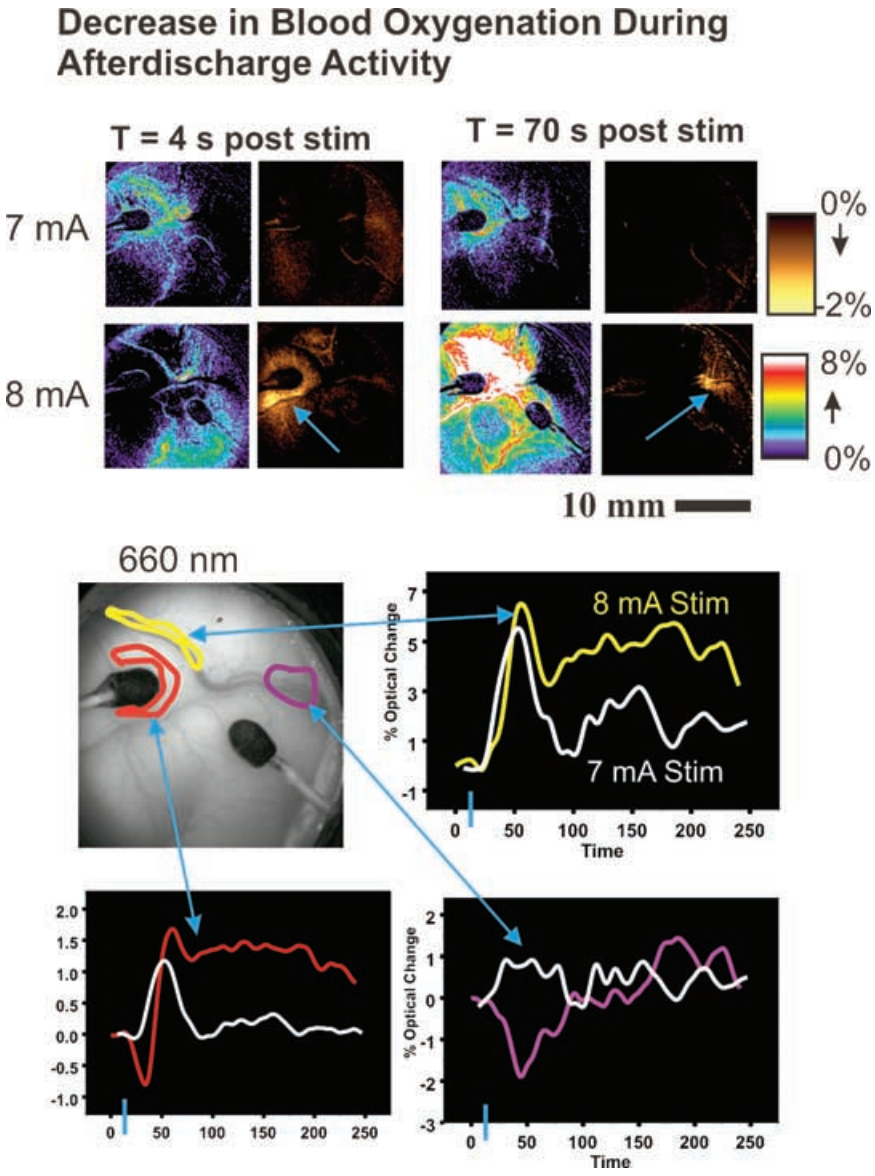

FIG. 4. Changes in Blood Oxygenation During Electrical Stimulation and Afterdischarge Activity. The top left panel of four images compares the optical changes between 7 mA stimulation (below the afterdischarge threshold) and 8 mA (above the afterdischarge threshold), at 4 seconds after the electrical stimulation had ceased, acquired from an individual animal. Images showing changes in the positive direction are shown in figures pseudo-colored with a "rainbow" spectrum, and images showing changes in the negative direction are pseudo-colored with a "gold" spectrum. At 7 mA, all changes are in a positive-going direction (top, left panel of four images), but at 8 mA, the area surrounding the electrode changes to a negative direction. More than a minute after stimulation-evoked and epileptiform activity had ceased, a localized area was seen to show a negative-going signal (top right panel of four images). In the bottom panel of figures, pixel values from within the regions indicated in the grey-scale images are plotted for comparison. The changes occurring during 7 mA stimulation (no afterdischarge activity) are plotted as white traces, and those at 8 mA (where afterdischarge activity occurred) are plotted in colors corresponding to their regions indicated in the grey-scale image.

to completely recover back to prestimulation baseline levels.

It has been noted that intense activation of the cortex with electrical stimulation evokes an initial "negative dip" at the 660 nm blood oxygenation wavelength (Fig. 3; Bottom, right; orange arrow). Further analysis of IOS-images acquired at this wavelength reveal a more complex pattern of positive and negative changes (Fig. 4). Although electrical stimulation at currents below the afterdischarge threshold sometimes elicit a small negative dip (20% of the 7 mA stimulation trials during the experiment shown), the negative dip is consistently observed during stimulation currents sufficient to evoke afterdischarge activity (Fig. 4; Top, left). The negative dip around the electrode always peaked within several seconds following stimulation, and was restricted to the tissue surrounding the stimulating electrode. In the experiment shown, stimulation at 8 mA consistently evoked 12–13 s of afterdischarge activity following the cessation of electrical stimulation. During stimulation trials in which such epileptiform activity occurred, optical images also showed negative-dips at later time points (20–60 s after all stimulation and afterdischarge activity had ceased) at sites more distant from the stimulating electrode (Fig. 4; top, right). These negative-dips were often localized within smaller veins. Quantification of the 660 nm optical data shows that both types of negative dips occurred in trials that involved stimulation above the afterdischarge threshold (and hence occurred in those trials in which 12–13s of epileptiform activity had been evoked).

Although early-occurring negative dips around the stimulating electrode were never observed at the 535 nm blood volume wavelength, the later-occurring negative dips were observed (Fig. 5A). At this wavelength, a

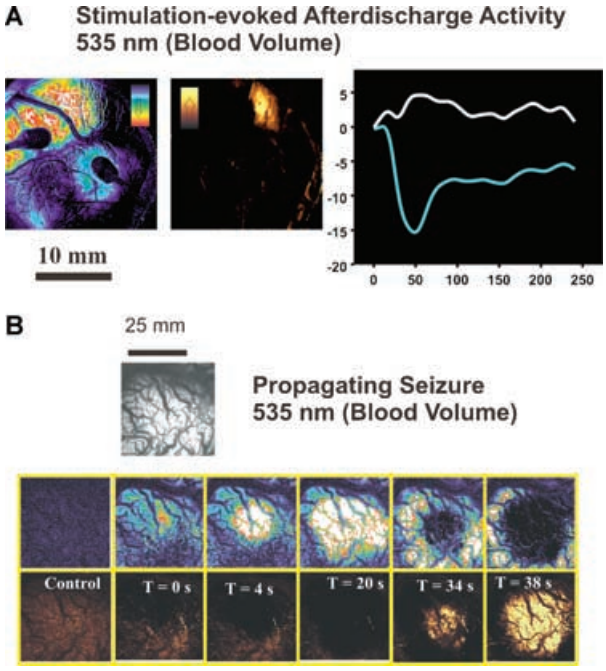

FIG. 5. Negative-going Optical Signals at the 535 nm Blood-Volume Wavelength. The images shown in **A** are from the same cortical area as shown in Fig. 4, but acquired under 535 nm light. The left two figures show positive (leftmost rainbow pseudo-colored image) and negative (gold pseudo-colored image) changes at 30 seconds following the cessation of electrical stimulation at 8 mA, at the end of the afterdischarge activity. The top right graph shows a plot of the optical changes (% optical change versus time in seconds), from a region surrounding the stimulating electrode (blue trace) to a region overlying the area of negative-going optical signal (white trace). The images shown in **B** were acquired during an ictal discharge spreading over the cortex. An acute seizure focus had been created by applying a 0.5 mm pledget soaked in bicuculline to the cortex for several minutes, directly in the center of the region shown in the image. A series of images are shown that were acquired during a spontaneous ictal discharge. The top line of rainbow pseudo-colored images show positive going signals, and the bottom series of gold pseudo-colored images show the negative going signals.

negative dip refers to a positive-going signal that may indicate a reduction of blood volume. These later-occurring dips at 535 nm were observed to occur within the tissue lying next to the same veins that had shown a negative dip at 660 nm.

More intense negative signals at the blood volume wavelength have been observed with more intense epileptiform activity (Fig. 5B). In experiments in which acute epileptic foci are created by focal application of bicuculline to the cortical surface, propagating waves of seizure activity can be imaged at the blood volume wavelength. After each ictal discharge is initiated, those regions of tissue lying just behind the traveling wave of neuronal activity eventually show a significant negative signal, suggesting the possibility that blood is being redistributed from regions that were previously highly active into areas undergoing a phase of increasing ictal activity.

DISSOCIATING BLOOD VOLUME FROM BLOOD OXYGENATION CHANGES WITH IOS

Many different arguments have been put forth in the literature justifying the interpretation of a certain wavelength as being more or less selective for blood volume or blood oxygenation (Nemoto et al., 1999; Mayhew et al., 2000; Lindauer et al., 2001; 2001; Haglund and Hochman, 2004). Our claim that 535 nm is specific for blood volume and 660 nm is specific for blood oxygenation is based on the direct observation of the optical changes occurring within the distinct microvascular compartments that are known to be the major players in the redistribution of blood during cortical activation. We showed that at 535 nm, the largest optical changes were negative-going and restricted to the dilating pial arterioles, and were largely absent from the venous network. In contrast, at 660 nm, the largest optical changes were positive-going, mostly restricted to the venous network, and were greatest in the larger macroscopic veins lying within the cortical sulci. Although these observations are consistent with respect to the predictions arising from consideration of the absorption spectra of oxy- and deoxy-hemoglobin presented earlier, we stress that this spectral-argument was meant as a rationale for choosing wavelengths, and not as a rigorous analysis. Although our data strongly suggests that IOS imaging can select for either blood volume of blood oxygenation, this in no way implies that a quantitative relationship has been established. That is, it is not known how a given percent change in the optical signal at either wavelength is correlated to the true absolute changes in blood volume or blood oxygenation.

An important observation is that optical measurements of blood volume appear to be much better localized to sites of neuronal activation than measurements of blood oxygenation. For example, 535 nm optical changes are localized within the tissue surround the stimulating electrode, whereas 660 nm changes are greatest within the larger veins at sites more distant from the stimulated tissue. A likely exception to this observation is the early-onset negative-going blood oxygenation change at 660 nm, which also appears to be localized to the tissue surround the stimulating electrode at higher stimulation currents. This is consistent with other observations that a negative-going blood oxygen-dependent signal is better localized to neuronal activity (Silva et al., 2000).

WAVELENGTH DEPENDENCY OF IOS IMAGING

As an experimental imaging technique, IOS imaging has no commonly adhered to standards, meaning that different investigators use a variety of different optical wavelengths in their experiments, from 500 nm through the near-infrared wavelengths greater than 800 nm (for examples, see: Grinvald et al., 1988; Haglund et al., 1992; Nemoto et al, 1999; Haglund and Hochman, 2004; Sheth

et al., 2003). The data shown here illustrates the difficulties in comparing results between similar experiments for data acquired at different wavelengths. For example, our early optical imaging study in human cortex (Haglund et al., 1992) was performed with a longpass 690 nm filter, and hence likely included a mixture of both blood volume and blood oxygenation signals (Fig. 1). Although such non-specific wavelengths are useful for localizing activity, their physiological interpretation is ambiguous.

INTERPRETATION OF "NEGATIVE" OPTICAL SIGNALS

Optical changes going in the opposite direction as to what is expected during increases in neuronal activity have been referred to a "negative signals," or "dips" (Malonek and Grinvald, 1996; Buxton, 2001). In the context of the data presented here, this means positive optical changes at 535 nm, suggesting a reduction in blood volume, and negative optical changes at 660 nm suggesting a decrease in blood oxygenation.

Much careful work has been published and debated on the interpretation of negative signals (Malonek and Grinvald, 1996; Buxton, 2001, Lindauer et al., 2001; Mayhew et al., 2001), and the data shown here is not meant to address the major open questions on this issue. Rather, our data are specific to the wavelengths and animal model used here, and in that context may provide some useful insights. It is important to keep in mind what is meant by a "negative optical signal": those optical changes that occur in an opposite direction to what is expected to be elicited by neuronal activation at a specific wavelength. Hence to avoid confusion, we describe these changes as "opposite-going" optical signals. There was a single type of opposite-going signal observed at the 535 nm blood volume wavelength. At low magnification, these optical changes were always observed to lie within the tissue (rather than larger vessels) at sites distant from the site of electrical stimulation. In the case of seizure spreading over the neocortex, these opposite-going blood volume signals were observed to lag immediately behind the wavefront of positive-going optical changes.

There were two types of opposite-going changes at the 660 nm blood oxygenation wavelength. The first type had an early onset and was restricted to the tissue surrounding the stimulating electrode. It may be that this type of opposite-going signal represents a deoxygenation of the tissue mediated by sufficiently intense electrical stimulation, an interpretation which has been previously proposed by other investigators (Malonek and Grinvald, 1996; Silva et al., 2000). The second type of opposite-going signal occurred some tens of seconds after cessation of the electrical stimulus and epileptiform activity. This signal occurred within veins overlying or next to regions that had shown opposite-going signals at 535 nm. It may be that this type of opposite-going signal is due to draining of deoxygenated blood arising from the more intense epileptiform activity that had occurred at some earlier time. Another possibility is that a sufficient reduction of blood volume mediated through localized blood stealing might allow for a deoxygenation of hemoglobin beyond what is normally observed.

NEOCORTICAL IOS IMAGING FOR STUDYING SEIZURE ACTIVITY IN ANIMAL MODELS: HOW WELL DO DIFFERENT SPECIES COMPARE TO EACH OTHER AND TO THE HUMAN?

Since the optical signals appear to be exquisitely sensitive to the redistribution and oxygen content of blood within the cortex, at least two factors suggest there may be significant species differences in the spatial and temporal dynamics of the optical signal: (i) scale and size of the neocortex, and (ii) species differences in cortical vascularization.

The surface area of the human neocortex is at least 10 times larger than the macaque monkeys used in our studies, and 15% thicker; compared to the mouse, the human cortex is 1000 times larger and twice as thick (Kaas, 2000; Striedter, 2005). The activation of a half-centimeter of cortex (for example) represents an insignificant fraction of the entire neocortex in the human, but a meaningful percentage in smaller animals. It might therefore be expected that phenomena such as blood stealing or deoxygenation, which generate opposite-going signals, might be more prevalent in smaller animals and have significantly different time courses and spatial patterns than what is observed in primates and humans. Indeed, a significant "epileptic dip" has been reported in some rat studies (Suh et al., 2005), but not observed in human studies (Haglund and Hochman, 2004, 2005) or in the primate studies reported here. Furthermore, synaptic activity preceding an epileptiform burst elicited by a pharmacological treatment might occur over a relatively large fraction of cortex in a small animal and be sufficient to generate hemodynamic changes and a corresponding optical signal (Chen et al., 2000) that may not be present in larger animals.

Species differences in neocortical vascularization may represent another important factor to consider in the interpretation of IOS imaging studies. There is some evidence to suggest dramatic phylogenic differences in the organization of the pial arterial network supplying the cortex (Mchedlishvili and Kuridze, 1984). Associated with increasing species development is a significant increase in the density and interconnectivity of the pial network. It has been suggested that these differences in neocortical vascularization determine the precision to which hemodynamic changes are correlated to neuronal activity, both spatially and temporally (Mchedlishvili, 1987). Since the

pial arterioles nearest the neuronal activity dilate, blood may be redistributed over a relatively larger surface area of the cortex in the sparser arterial network of a rat than in a denser and more interconnected network of a cat, and much more so than in a primate (Mchedlishvili and Kuridze, 1984). The differential effects of species variation in cortical vascularization on the optical signal may be amplified by intense and prolonged neuronal discharging, such as what might be associated with various pharmacological seizure models.

The potential differences between species in the hemodynamic-related optical signals suggest that caution is required in the interpretation and comparison of IOS-imaging data acquired from different seizure models. It may not be straightforward to generalize results addressing hemodynamic regulation and blood oxygenation during epileptiform activity obtained from smaller animals, such as rats and mice to the human. However, IOS imaging in smaller animals may have other important uses, such as for comparing the magnitude of the effects of various treatments on epileptiform activity.

COMPARING IOS IMAGING TO OTHER IMAGING MODALITIES

IOS imaging is strictly limited to detecting hemodynamic changes occurring at the cortical surface, but with micron-level spatial resolution and sufficiently high sensitivity to measure changes occurring within individual microscopic vessels. Studies using other modalities, such as BOLD-fMRI, typically report changes from deeper structures or integrate changes occurring within larger volumes of cortex with different spatial resolutions and sensitivities (Kobayashi et al., 2006). Although some studies have been performed that directly compared neocortical optical changes and BOLD-fMRI signals (Strangman et al., 2002), more work is required to better explain the differences between data acquired with optical imaging and other non-optical imaging modalities.

FUTURE DIRECTIONS

Two lines of further research may provide further insight into the interpretation of IOS imaging that would increase its usefulness as an experimental tool. The first is to better understand the relationships between optical changes and neuronal activity (both action potential firing, and excitatory and inhibitory synaptic activity). Although numerous studies have provided some information on these relationships (Grinvald et al., 1988), more precise information may be obtained from studies using newer technologies. Such technologies might include the use of fast, sensitive cameras, or photodiode arrays with sufficiently high spatial resolution to map real-time changes using voltage-sensitive dyes for comparison to the IOS (Ma et al., 2004). A second area of future investigation is in establishing the quantitative correlations between absolute changes in blood oxygenation and blood volume to optical signals acquired at selective wavelengths.

REFERENCES

Buxton RB. (2001) The elusive initial dip. *NeuroImage* 13: 953–958.

Cannestra AF, Pouratian N, Bookheimer SY, Martin NA, Beckerand DP, Toga AW. (2001) Temporal spatial differences observed by functional MRI and human intraoperative optical imaging. *Cereb Cortex* 11:773–782.

Chen JW, O'Farrell AM, Toga AW. (2000) Optical intrinsic signal imaging in a rodent seizure model. *Neurology* 55:312–315.

Fox PT, Raichle ME. (1986) Focal physiological uncoupling of cerebral blood flow and oxidative metabolism during somatosensory stimulation in human subjects. *Proc Natl Acad Sci USA* 83:1140–1144.

Fung, YC. (1997) *Biomechanics: circulation* Springer, New York.

Grinvald, A. (1992) Optical imaging of architecture and function in the living brain sheds new light on cortical mechanisms underlying visual perception. *Brain Topogr* 5:71–75.

Grinvald A, Frostig RD, Lieke E, Hildesheim R. (1988) Optical imaging of neuronal activity. *Physiol Rev* 68: 1285–1366.

Haglund MM, Hochman DW. (2004) Optical imaging of epileptiform activity in human neocortex. *Epilepsia* 45(Suppl 4): 43–47.

Haglund MM, Hochman DW. (2005) Furosemide and mannitol suppression of epileptic activity in the human brain. *J Neurophysiol* 94:907–918.

Haglund MM, Ojemann GA, Blasdel GG. (1993) Optical imaging of bipolar cortical stimulation. *J Neurosurg* 78:785–793.

Haglund MM, Ojemann GA, Hochman DW. (1992) Optical imaging of epileptiform and functional activity in human cerebral cortex. *Nature* 358: 668–671.

Holthoff K, Witte OW. (1996) Intrinsic optical signals in rat neocortical slices measured with near-infrared dark-field microscopy reveal changes in extracellular space. *J Neurosci* 16: 2740–2749.

Iadecola C. (2004) Neurovascular regulation in the normal brain and in Alzheimer's disease. *Nat Rev Neurosci* 5:347–360.

Kaas J.H. (2000) Why is brain size so important. *Brain and Mind* 1:7–23.

Kobayashi E, Bagshaw AP, Benar CG, Aghakhani Y, Andermann F, Dubeau F, Gotman J. (2006) Temporal and extratemporal BOLD responses to temporal lobe interictal spikes. *Epilepsia* 47:343–354.

Lindauer U, Royl G, Leithner C, Kuhl M, Gold L, Gethmann J, Kohl-Bareis M, Villringer A, Dirnagl U. (2001) No evidence for early decrease in blood oxygenation in rat whisker cortex in response to functional activation. *Neuroimage* 13:988–1001.

Ma HT, Wu CH, Wu JY. (2004) Initiation of spontaneous epileptiform events in the rat neocortex in vivo. *J Neurophysiol* 91:934–945.

MacVicar BA, Hochman D. (1991) Imaging of synaptically evoked intrinsic optical signals in hippocampal slices. *J Neurosci* 11: 1458–1469.

Malonek D, Grinavald A. (1996) Interactions between electrical activity and cortical microcirculation revealed by imaging spectroscopy: implications for functional brain mapping. *Science* 272:551–554.

Malonek D, Grinvald A. (1997) Vascular regulation at sub millimeter range. Sources of intrinsic signals for high resolution optical imaging. *Adv Exp Med Biol* 1997;413:215–220.

Martin, KA (2002) Microcircuits in visual cortex. *Curr Opin Neurobiol* 12:418–425.

Mayhew J, Johnston D, Berwick J, Jones M, Coffey P, Zheng Y. (2000) Spectroscopic analysis of neural activity in brain: increased oxygen consumption following activation of barrel cortex. *Neuroimage* 12:664–675.

Mayhew J, Johnston D, Martindale J, Jones M, Berwick J, Zheng Y. (2001) Increased oxygen consumption following activation of brain: theoretical footnotes using spectroscopic data from barrel cortex. *Neuroimage*. 13:975–987.

Mchedlishvili G. (1987) *Arterial behavior and blood circulation in the brain*. Plenum Press, New York.

Mchedlishvili G, Kuridze N. (1984) The modular organization of the pial arterial system in phylogeny. *J Cereb Blood Flow Metab* 4:391–396.

Nemoto M, Nomura Y, Sato C, Tamura M, Houkin K, Koyanagi I, Abe H. (1999) Analysis of optical signals evoked by peripheral nerve stimulation in rat somatosensory cortex: dynamic changes in hemoglobin concentration and oxygenation. *J Cereb Blood Flow Metab* 19:246–259.

Ngai A, Ko KR, Morii S, Winn HR. (1988) Effect of sciatic nerve stimulation on pial arterioles in rats. *Am J Physiol* 254:H133-H139.

Roland PE. (1997) *Brain activation* Wiley-Liss, New York.

Sato K, Nariai T, Tanaka Y, Maehara T, Miyakawa N, Sasaki S, Momose-Sato Y, Ohno K. (2005) Functional representation of the finger and face in the human somatosensory cortex: intraoperative intrinsic optical imaging. *Neuroimage* 25:1292–1301.

Schummers, J., Marino, J., Sur, M. (2004) Local networks in visual cortex and their influence on neuronal responses and dynamics. *J Physiol Paris* 98:429–441.

Schwartz TH, Bonhoeffer T. (2001) In vivo optical mapping of epileptic foci and surround inhibition in ferret cerebral cortex. *Nat Med* 7:1063–1067.

Schwartz TH, Chen LM, Friedman RM, Spencer DD, Roe AW. (2004) Intraoperative optical imaging of human face cortical topography: a case study. *Neuroreport* 15:1527–1531.

Sheth S, Nemoto M, Guiou M, Walker M, Pouratian N, Toga AW. (2003) Evaluation of coupling between optical intrinsic signals and neuronal activity in rat somatosensory cortex. *Neuroimage* 19: 884–894.

Silva AC, Lee SP, Iadecola C, Kim SG. (2000) Early temporal characteristics of cerebral blood flow and deoxyhemoglobin changes during somatosensory stimulation. *J Cereb Blood Flow Metab* 20:201–206.

Strangman G, Culver JP, Thompson JH, Boas DA. (2002) A quantitative comparison of simultaneous BOLD fMRI and NIRS recordings during functional brain activation. *Neuroimage* 17:719–731.

Striedter GF. (2005) *Principles of Brain Evolution*. Sinauer Associates, Inc., MA.

Suh M, Bahar S, Mehta AD, Schwartz TH. (2005) Temporal dependence in uncoupling of blood volume and oxygenation during interictal epileptiform events in rat neocortex. *J Neurosci* 25:68–77.

Tanaka, K. (2000) Mechanisms of visual object recognition studied in monkeys. *Spat Vis* 13:147–163.